Molecular BioSystems

Accepted Manuscript

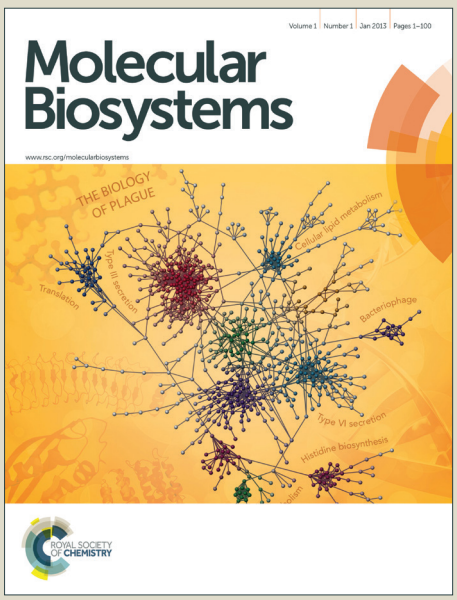

ROYAL SOCIETY OF CHEMISTRY

www.rsc.org/molecularbiosystems

Table of contents:

This study identified the potential biomarkers in urine, plasma and feces of high fructose-fed rats by using ^{1}H NMR-based metabonomics.

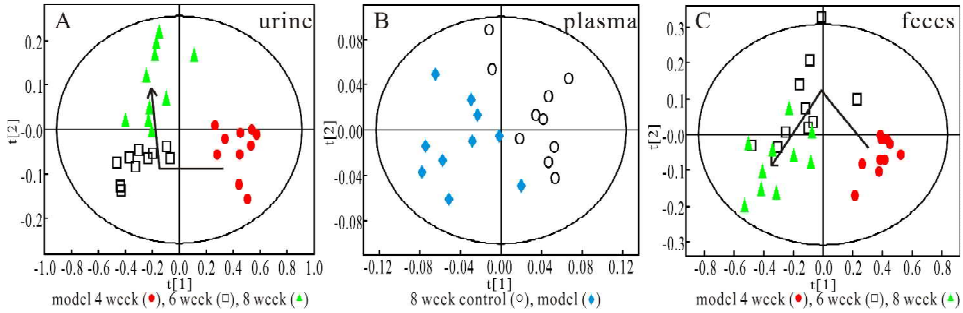

An integrated metabonomic approach to study metabolic profiles in insulin resistance rat model induced by high fructose

Yongxia Yang [a*], *Linlin Wang*[a, b#], *Shumei Wang*[b], *Rongbo Huang*[a], *Lingyun Zheng*[a], *Shengwang Liang*[b], *Lei Zhang*[a], *Jingfen Xu*[a]

[a] School of Basic Courses, Guangdong Pharmaceutical University, Guangzhou, 510006, P. R. China

[b] Department of Traditional Chinese Medicine, Guangdong Pharmaceutical University, Guangzhou, 510006, P. R. China

***Corresponding author:**

Associate Prof. Yongxia Yang: School of Basic Courses, Guangdong Pharmaceutical University, Guangzhou, 510006, P. R. China; Tel: 86-(0)20-3935-2197, Fax: 86-(0)20-3935-2186, E-mail: sheepma@163.com

[#] contributed equally to this work.

Abstract

Insulin resistance (IR) is one of the common risk factors for the development of metabolic diseases, and gradually becomes a hot issue of research. It was reported that excessive feeding of high fructose induced insulin resistance for both humans and rats. The aim of this study was to investigate the progression of IR and identify potential biomarkers in urine, plasma and fecal extracts of high fructose-fed rats by using ^{1}H NMR-based metabonomics approach. The biochemical analysis was also performed. The plasma levels of pyruvate and lactate in the IR model rats reduced significantly, as well as the decrease of citrate and α-KG in urine and succinate in fecal, suggesting the perturbation of energy metabolism. The decreased level of taurine in urine and fecal extracts during the whole experiment, together with increased urinary level of creatine/creatinine revealed liver and kidney injury. Decreased levels of choline containing metabolites in urine and increased level of betaine in urine and plasma demonstrated altered transmethylation. The changes of hippurate, acetate, propionate and n-butyrate suggested the disturbance of intestinal flora in IR rats. This study indicated that ^{1}H NMR-based metabonomics can provide biochemical information for the progression of IR and offers a non-invasive means to the discovery of potential biomarkers.

Key words: ^{1}H NMR; Metabonomics; Insulin resistance; Fructose; Pattern recognition

1. Introduction

The incidence and prevalence of insulin resistance (IR) associated diseases are occurring at alarmingly increasing rates with frightful consequences to the health of human worldwide.[1] Insulin resistance, the decreased response of peripheral tissue to normal insulin levels, is known as the underlying cause of type 2 diabetes mellitus (DM), cardiovascular disease and metabolic syndrome (MS).[2] One of the main driving forces for the increased prevalence of MS is modern westernized diets associated with the dramatic rises in obesity. Diets high in saturated fats and fructose have been shown to induce weight gain, insulin resistance and hyperlipidemia in humans and animals.[3,4] For thousands of years humans have consumed fructose from its natural sources, i.e. fresh fruits and vegetables, in a range of 16-20 g per day. However, the significant increase in added fructose from Westernized diets has increased the daily consumptions amounting to 85-100 g of fructose per day.[5] It has been postulated that such increased consumption would contributed to obesity, type 2 diabetes and MS.[6] Studies have showed that administration of a high fructose diet to normal rats induced IR and MS.[7-9] Human studies have also reported that dietary fructose may increase caloric intake and, consequently, obesity and the associated features of MS.[10]

Metabolic disorders were common in IR-correlated diseases including DM and hyperlipidemia. Cannizzob [11] et al. reported that high fructose induced a marked increase in plasma glucose, insulin and triglycerides, provoked vascular remodeling and enlarged atherosclerotic lesion in aortic and carotid arteries. High fructose diet can also induce severe liver steatosis, with significantly higher cholesterol level.[12] Therefore, research of metabolic changes of fructose-induced IR rat models is most important for understanding the metabolic mechanism for IR-based metabolic diseases.

With the development of new analytical techniques, metabonomics offers an alternative method for monitoring the biochemical changes induced by endogenous and exogenous factors,[13,14] which was proved to be an effective and nondestructive method to probe the metabolic responses within a whole organism. In conjunction with pattern recognition (PR) data analysis techniques, such as principal component analysis (PCA) and partial least squares projection on discriminant analysis (PLS-DA), NMR-based metabonomics has been widely applied in many metabolic diseases.[15,16]

In this study, we established the IR model induced by feeding of 10% fructose drinking water, similar with the modeling method preciously reported.[17] The aim of this research is to investigate the time-dependent metabolic changes of IR model by an integrated metabonomic approach on urine, plasma and feces. Meanwhile, the blood glucose level and IR index were determined by biochemistry methods.

2. Materials and Methods

2.1 Animal experiment and sample collection

Twenty male Wistar rats (weighting 180-200g) were purchased from Medical Laboratory Animal Center of Sun Yat-Sen University, and housed in a well-ventilated animal experimental laboratory, with a 12 h light/dark cycle, a temperature of 25 ± 1 °C, and a relative humidity of 50±10%. This study was reviewed and approved by the Ethics Committee of Guangdong Pharmaceutical University. Food and pure water were freely provided. After acclimatization for one week, the rats were randomly divided into two groups (n=10/group), i.e. control group and fructose-fed group. The control rats were administrated with distilled water for 8 weeks. The model rats were consecutively fed with 10% fructose water in the whole procedure for 8 weeks. This IR modeling method was according to the method of Mahmoud.[17]

During the experimental period, feces and urine samples of each group were collected at the end of 4th, 6th and 8th week. Urine sample collection was carried out overnight for 12h using metabolism cages. 100 ul of 1% Sodium azide was pipetted into collection container for anti-bacteria before urine collection. Fecal samples were taken immediately prior to the rats being removed from the metabolic cages. All the samples were stored at -80°C for NMR determination. Blood samples were collected by orbital venous plexus at the end of 4th week just for clinical chemistry analysis after fasting for 12 h. In addition, plasma samples at the end of 8th week were collected for clinical chemistry analysis and NMR analyses.

2.2 Sample preparation

2.2.1 Urine and plasma samples preparation

The urine and plasma samples were thawed at room temperature just prior to NMR analysis. 300 μL of sample was mixed with 200 μL of phosphate buffer (0.2 M Na_2HPO_4/ NaH_2PO_4, pH 7.4) to minimize chemical shift variations and then centrifuged (14,000 g, 10 min, 4 °C) to remove any precipitates. The supernatant was then pipetted into 5 mm NMR tube and 80 μL of D_2O containing 0.05% sodium 3-trimethylsilyl-(2, 2, 3, 3-$^2H_4$)-1-propionate (TSP) was added.

2.2.2 Fecal extracts preparation

Fecal extract method for NMR analyses was referenced to the reported result by Y Zhao.[18] Briefly, fecal extracts were prepared by mixing 70 mg of fecal samples with 700 μL of phosphate buffer (0.1 M Na_2HPO_4/NaH_2PO_4 = 4/1, pH = 7.4).

After vortex mixing, the samples were subjected to freeze-thaw treatments for 3 times and followed with ultrasonication cycles for 10 times, then collected the supernatant. The residuals were subjected to the extract method mentioned above once again. The supernatants were merged and centrifuged (14,000 g, 10 min, 4 °C). 400 μL of

supernatant was transferred into 5 mm NMR tube and 100 μL of D_2O containing 0.05% sodium 3-trimethylsilyl-(2, 2, 3, 3-$^2H_4$) -1-propionate (TSP) was added.[18]

2.3 ^{1}H NMR spectroscopy

^{1}H NMR spectra of all samples were collected at 298K on a Bruker Avance III 500 MHz spectrometer. The ^{1}H NMR spectra of urine and fecal extracts samples were recorded using the water-presaturated standard one-dimensional NOESYPR1D pulse sequence (recycle delay-90°-t_1-90°-t_m-90°-acquisition) for representation of the total metabolite compositions. 64 transients were collected into 32k data points using a spectral width of 10 kHz with a relaxation delay of 3 s, and mixing time (t_m) of 100 ms. t_1 was set to 3 μs. The ^{1}H NMR spectra of plasma samples were recorded using the water-suppressed standard one-dimensional Carr-Purcell-Meiboom-Gill (CPMG) spin-echo pulse sequence (RD-90°-(τ-180°-τ)$_n$-acquisition) in order to reduce the peaks overlapping. 128 transients were collected into 32k data points using a spectral width of 10 kHz with a relaxation delay of 3 s, and total echo time was 100 ms. The free-induction decays (FIDs) were multiplied by an exponential function with a line-broadening factor of 0.3 Hz before Fourier transformation. The chemical shifts of spectra were referenced to the TSP at δ 0.00.

2.4 Pattern recognition and statistical analysis

All the spectra were phase- and baseline-corrected manually, and then bucketed and automatically integrated with an automation routine in AMIX. Each ^{1}H NMR spectrum was segmented into regions of 0.005 ppm (plasma and urine) or 0.02 ppm (fecal extracts). The region of δ 4.6-5.2 was discarded to eliminate the effects of water suppression. The integrals of these buckets covered the region δ 0.5-9.0 and were normalized to the total sum of the spectral integrals, as variables for PCA and

PLS-DA. For urine spectra, the region containing urea (δ 5.2-6.2) was also discarded to eliminate the urea signals.

All ^{1}H NMR spectra were submitted to PCA and PLS-DA using the software Simca-P^{+} 12.0 (Umetrics, Sweden). Scores plots, highlighting inherent clustering trends of the samples, and loadings plots, providing potential biomarkers, were visualized. Statistical analyses were performed with an analysis of variance. A $p<0.05$ was considered significant.

2.5 Weight measurement, blood glucose and IR index assessment

At the end of 4th and 8th week, the weight of each rat was measured. Fasting blood glucose was determined colorimetrically by using a Randox reagent kit, according to the method of Barham and Trinderb.[19] Blood insulin levels were assayed with a sandwich ELISA (Millipore), which used a microtiter plate coated with mouse monoclonal anti-rat insulin antibody. The homeostasis model assessment for insulin resistance index was calculated according to the following equation:[20]

HOMA-IR= glucose concentration (mmol/L)×insulin (mU/L)/22.5.

Independent sample *t* test was conducted to compare the biochemical data of IR model rats and control rats.

3. Results

3.1 Influence of fructose feeding on weight, blood glucose and insulin resistance

The fructose feeding had induced weight gain at the end of 4th and 8th week (Table 1), while it had no obvious influence on blood glucose, which was similar with the results reported.[17] IR index increased after 4 weeks fructose feeding and continued to elevate at the end of 8th week with statistical significance. So fructose feeding had induced insulin resistance successfully.

Table 1 Summary of weight, glucose level and IR index data at the end of 4th and 8th week.

Group	4th week			8th week		
	Weight (g)	Glucose (mmol/L)	IR	Weight (g)	Glucose (mmol/L)	IR
Control	314.43±7.44	4.84±0.73	4.80±0.13	406.12±8.58	4.92±0.43	4.95±0.65
Model	343.87±18.61*	5.24±0.84	7.55±0.31*	464.45±22.43*	5.26±0.49	10.32±0.37**

Values are presented as means ± SD. *: to compare with controls * $p<0.05$; ** $p<0.01$.

3.2 ^{1}H NMR Spectroscopy and pattern recognition analysis of urine

Figure 1 showed the representative 500 MHz urinary ^{1}H NMR NOESYPR1D spectra of rats from control and fructose-fed IR group at the end of 8th week. Assignments of endogenous metabolites involved in ^{1}H-NMR spectra were based on the literature[21] and confirmed by 2D spectroscopy. The urinary NMR spectra were dominated by 2-hydroxybutyrate, isoleucine, leucine, valine, 3-hydroxybutyrate, lactate, alanine, acetate, N-acetylglycoprotein, acetone, acetoacetate, succinate, α-ketoglutaric acid (α-KG), citrate, dimethylglycine (DMG), creatine/creatinine, tyrosine, choline, PC/GPC, TMAO/betaine, taurine, glycine, glycerol, α-glucose, β-glucose, phosphoethanolamine, hippurate, fumarate, 4-hydroxyphenylactate, phenylacetylglycine and formate. Visually, the urinary metabolic profiles did not showed obvious discrimination between these two groups. Therefore, we did the multivariate data analysis to obtain the metabolic markers in IR models.

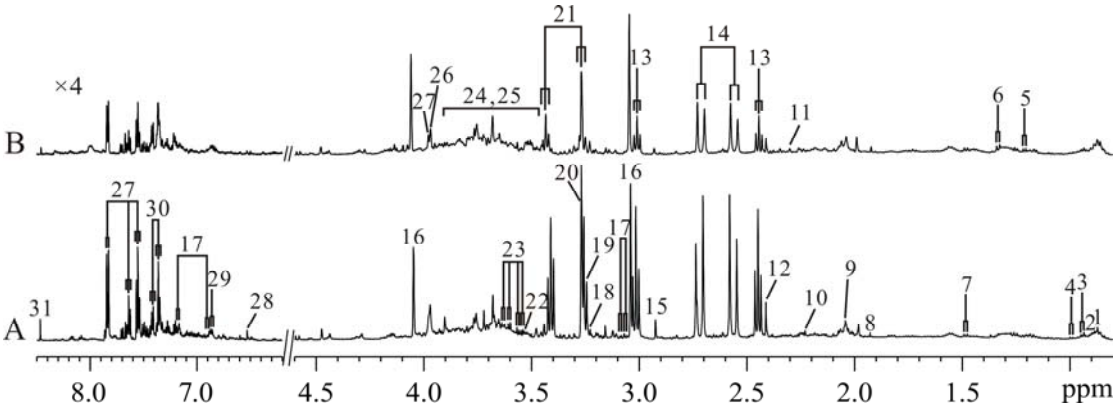

Figure 1 Representative urine ^{1}H NMR spectra from A: controls, B: fructose-fed IR rats at the end of 8th week. Keys: 1. 2-hydroxybutyrate; 2. isoleucine; 3. leucine; 4. valine; 5. 3-hydroxybutyrate; 6. lactate; 7. alanine; 8. acetate; 9. N-acetylglycoprotein; 10. acetone; 11. acetoacetate; 12.

succinate; 13. α-ketoglutaric acid (α-KG); 14.citrate; 15. dimethylglycine (DMG); 16.creatine/creatinine; 17. tyrosine; 18. choline; 19. PC/GPC; 20. TMAO/betaine; 21. taurine; 22. glycine; 23. glycerol; 24. α-glucose; 25. β- glucose; 26. phosphoethanolamine; 27. hippurate; 28. fumarate; 29. 4-hydroxyphenylactate; 30. phenylacetylglycine; 31. formate.

Figure 2A1 showed the score plot of PCA representing the distribution of all the urinary samples at the end of 4^{th} (●), 6^{th} (□) and 8^{th} (▲) week in IR group. It could be seen that there were obvious distribution trajectory of samples, as the arrow showed. With the increase of feeding time, the distribution of samples moved from right to left along t1 dimension, and then moved upward along t2 dimension. It might be concluded from the analysis results that urine metabolic profiles could reflect the metabonomic perturbations at different feeding time. PCA was also performed on the spectra data of control rats. The score plot didn't show obvious classification for the samples at three time points (Fig. 2A2). The PCA results revealed that metabolic variations in model rats were closely correlated with high fructose feeding.

PLS-DA models were established respectively for the classification between controls and fructose-fed IR rats in order to further detect the associated potential biomarkers. The distinct classifications between controls and IR rats at 4^{th}, 6^{th} and 8^{th} week were shown in the score plots (Fig. 2B1, C1 and D1). From the coefficient –coded loading plot (Fig. 2B2), it was found the levels of acetate, TMAO/betaine and creatine/creatinine increased, while citrate, α-KG and taurine decreased in the samples of fructose-fed models at the end of 4^{th} week. In addition to the metabolic changes mentioned above, the increased level of hippurate and decreased levels of choline and PC/GPC was found at the end of 6^{th} week (Fig. 2C2), while the changes of acetate, TMAO/betaine and hippurate were not evident at the end of 8^{th} week (Fig. 2D2).

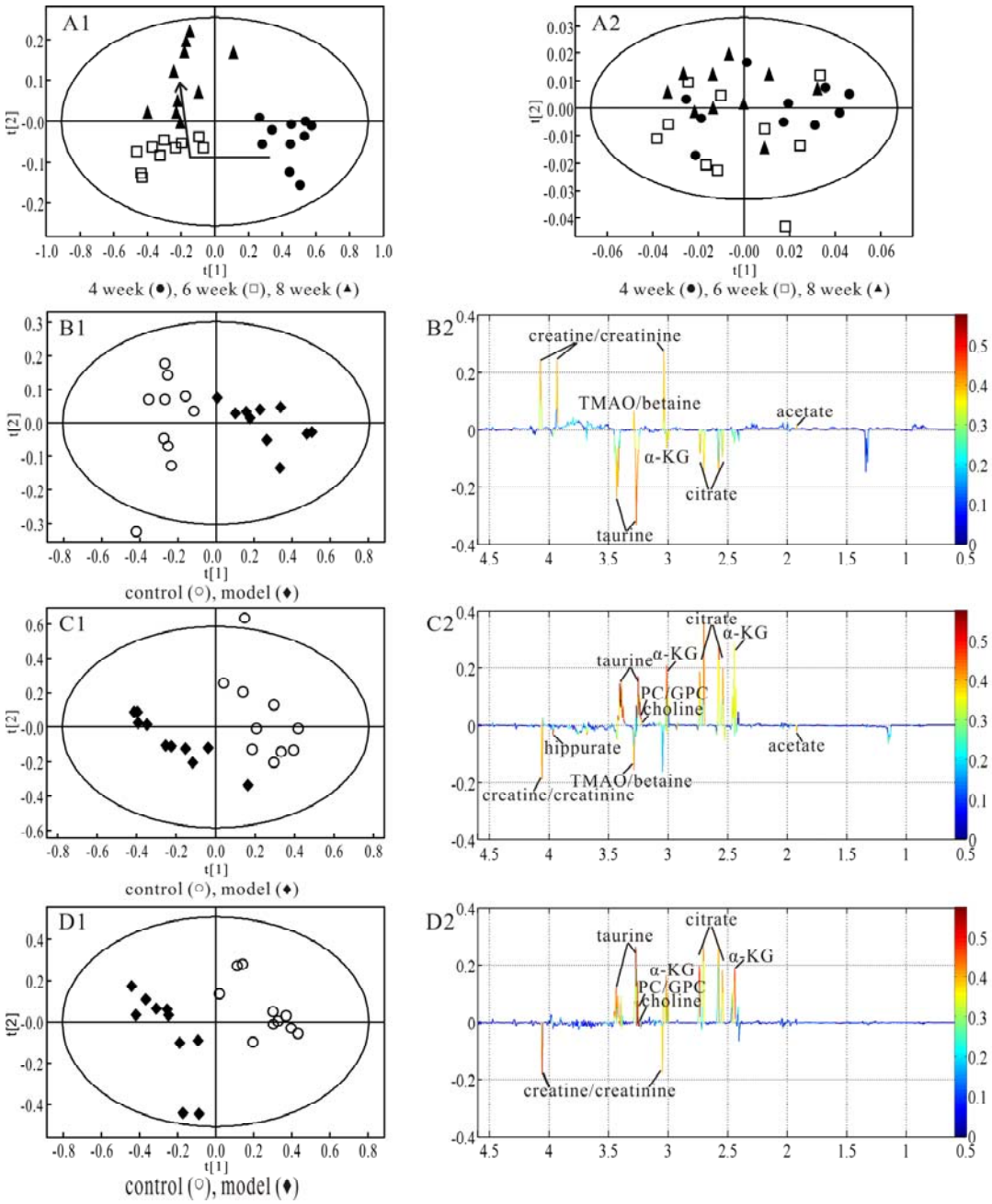

Figure 2 Multivariate analyses of urinary ^{1}H NMR spectra data at the end of 4th, 6th and 8th week. A1, A2: PCA score plots of IR model (R^2X=73.1%, Q^2=50.1%) and control (R^2X=75.4%, Q^2=45.3%) rats at three time points, respectively. B1, B2: Score plot and coefficient-coded loading plot of PLS-DA between control and model groups at the end of 4th week (R^2X=53.8%, Q^2Y=62.5%). C1, C2: Score plot and coefficient-coded loading plot of PLS-DA between control and model groups at the end of 6th week (R^2X=68.8%, Q^2Y=79.4%). D1, D2: Score plot and coefficient-coded loading plot of PLS-DA between control and model groups at the end of 8th week (R^2X=67.2%, Q^2Y=84.6%).

Table 2 summarized the statistical analysis results of the normalized integrals of metabolites screened out in Fig. 2, accounting for the metabolites differentiation between two groups at the end of 4^{th}, 6^{th} and 8^{th} week.

Table 2 The statistical analysis results of the metabolites in urine of IR model group at the end of 4^{th}, 6^{th} and 8^{th} week.

metabolites	chemical shift	variations		
		4^{th} week	6^{th} week	8^{th} week
acetate	1.92(s)	$\uparrow^{*}$	$\uparrow^{*}$	-
α-KG	2.45(t)	$\downarrow^{*}$	$\downarrow^{**}$	$\downarrow^{**}$
	3.01(t)			
citrate	2.56(d)	$\downarrow^{*}$	$\downarrow^{**}$	$\downarrow^{**}$
	2.72(d)			
creatine/creatinine	3.03(s)	$\uparrow^{*}$	$\uparrow^{*}$	$\uparrow^{**}$
	4.05(s)			
choline	3.21(s)	-	$\downarrow^{*}$	$\downarrow^{**}$
PC/GPC	3.23(s)	-	$\downarrow^{*}$	$\downarrow^{**}$
taurine	3.27(t)	$\downarrow^{*}$	$\downarrow^{**}$	$\downarrow^{**}$
	3.43(t)			
TMAO/betaine	3.27(s)	$\uparrow^{*}$	$\uparrow^{*}$	-
hippurate	3.97(s)	-	$\uparrow^{*}$	-

*: to compare with controls * $p<0.05$; ** $p<0.01$.

3.3 ^{1}H NMR spectroscopy and pattern recognition analysis of plasma

Two typical ^{1}H CPMG NMR spectra of plasma from control and model rats at 8^{th} week were shown in Fig.3. The NMR resonances were assigned according to the literature[22] and confirmed by 2D spectroscopy. We observed the metabolites including lipids, amino acids (leucine, isoleucine, valine, alanine and lysine), lactate and glucose, etc. The score plot of PLS-DA (Fig.4A1) showed the clear separation between the controls and IR rats. From the coefficient-coded loading plot (Fig.4A2), the elevated levels of lipid (mainly LDL/VLDL), alanine, acetate, taurine, TMAO/betaine and glycine, as well as decline in the levels of lactate, pyruvate and glycerol, were found in the plasma samples of IR models at the end of 8^{th} week.

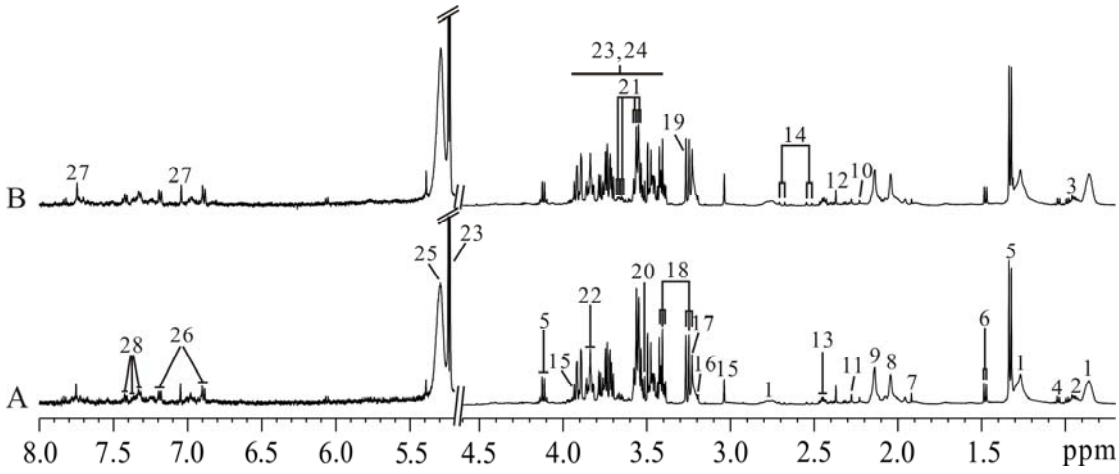

Figure 3 Representative plasma ^{1}H NMR spectra from A: controls, B: fructose-fed IR rats at the end of 8th week. Keys: 1. Lipid (mainly LDL/VLDL); 2. isoleucine; 3. leucine; 4. valine; 5. lactate; 6. alanine; 7. acetate; 8. N-acetyl glycoprotein; 9. O-acetyl glycoprotein; 10. acetone; 11. acetoacetate; 12. pyruvate; 13. glutamine; 14. citrate; 15. creatine/creatinine; 16. choline; 17. GPC/PC; 18. taurine; 19. TMAO/betaine; 20. glycine; 21. myo-inositol; 22. glycerol; 23. α-glucose; 24. β-glucose; 25. unsaturated lipid; 26. tyrosine; 27. 1-methylhistidine; 28. phenylalanine.

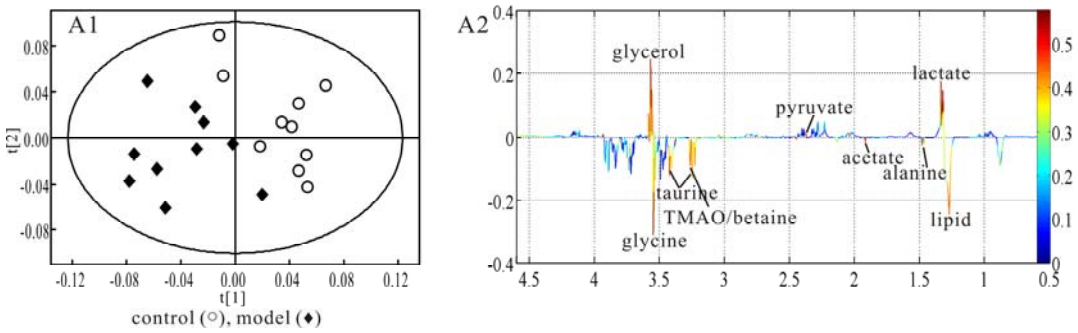

Figure 4 PLS-DA of plasma ^{1}H NMR spectra data from control and fructose-fed IR rats at the end of 8th week (R^2X=66.4%, Q^2Y=49.5%). A1: score plot; A2: coefficient-coded loading plot.

Table 3 summarized the statistical analysis results of the metabolites screened out in Fig. 4, accounting for the differentiation between two groups at 8th week.

Table 3 The statistical analysis result of the metabolites in plasma of control and model group at 8th week.

metabolites	chemical shift	variations 8th week
lipid	1.27(m)	↑**
lactate	1.33(d)	↓**
alanine	1.48(d)	↑*
acetate	1.92(s)	↑**
pyruvate	2.37(s)	↓*
TMAO/betaine	3.27(s)	↑**
taurine	3.43(t)	↑*
glycine	3.54(s)	↑*
glycerol	3.56(dd)	↓**

*: to compare with controls * $p<0.05$; ** $p<0.01$.

3.4 ^{1}H NMR Spectroscopy and pattern recognition analysis of fecal extracts

Fig.5 showed typical ^{1}H NMR NOESYPR1D spectra of fecal extracts from control and model rats at 8th week. Assignments of the metabolites involved in ^{1}H NMR spectra were based on the literatures[18,23] and confirmed by 2D spectroscopy. We observed that the main metabolites in the fecal extracts spectra were short chain fatty acids (SCFAs) such as butyrate, propionate and acetate, amino acids (leucine, isoleucine, valine, alanine and lysine), uracil, lactate and glucose and so on. In order to further find out the potential metabolic markers of IR models, we did the multivariate data analysis.

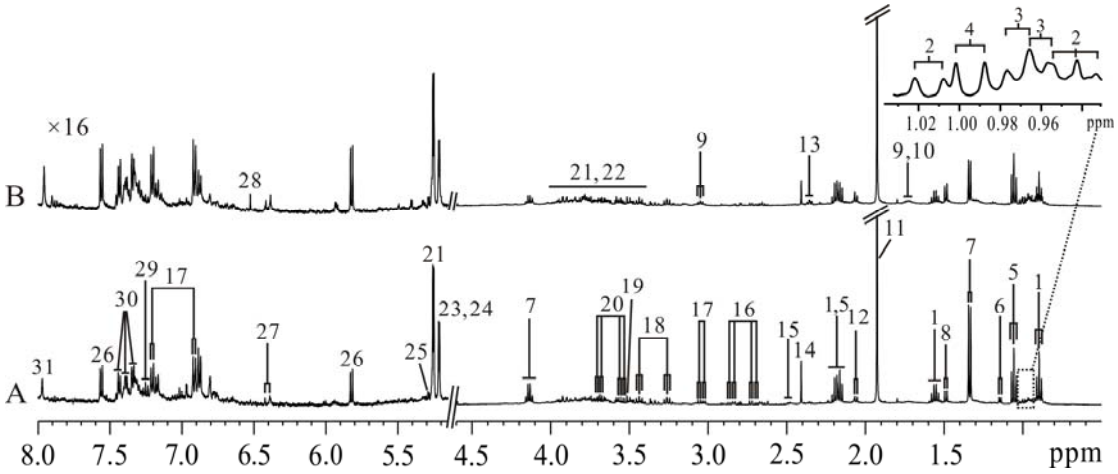

Figure 5 Representative ^{1}H NMR spectra of fecal extracts from A: controls, B: fructose-fed IR rats at the end of 8th week. Keys: 1. n-butyrate; 2. isoleucine; 3. leucine; 4. valine; 5. propionate; 6. α-ketoisovalerate; 7. lactate; 8. alanine; 9. lysine; 10. cadaverine; 11. acetate; 12. isobutyrate; 13.

glutamate; 14. succinate; 15. glutamine; 16. aspartate; 17. tyrosine; 18. taurine; 19. glycine; 20. glycerol; 21. α-glucose; 22. β-glucose; 23. α-xylose; 24. α-arabinose; 25. α-galactose; 26. uracil; 27. urocanate; 28. fumarate; 29. tryptophan; 30. phenylalanine; 31. histidine.

The score plot of PCA represented distribution of the model rats (Fig.6A1), where the samples at 4^{th} week were separated from the ones at 6^{th} and 8^{th} week along t1 dimension. A classification between 6^{th} and 8^{th} week was also observed as the arrow indicated, whereas the control group displayed no significant differences at three time points (Fig. 6A2). The PCA results indicated that metabolic variations in model rats could reflect the influence of fructose feeding.

PLS-DA models were established respectively for the classification between controls and fructose-fed IR rats in order to further detect the associated potential biomarkers respectively. The obvious classifications between controls and IR rats at 4^{th}, 6^{th} and 8^{th} week were shown in the score plots (Fig. 6B1, C1 and D1). From the coefficient-coded loading plot (Fig. 6B2), it was found the levels of alanine and glutamate increased, while n-butyrate, acetate, succinate and taurine decreased in the samples of fructose-fed models at the end of 4^{th} week. It was noted that the increased levels of n-butyrate and isobutyrate, as well as decreased levels of propionate, lactate and glycerol, were found at the end of 6^{th} week (Fig. 6C2). It was also found that isoleucine/leucine decreased in model rats at the end of 8^{th} week, while the change of succinate was not obvious (Fig. 6D2).

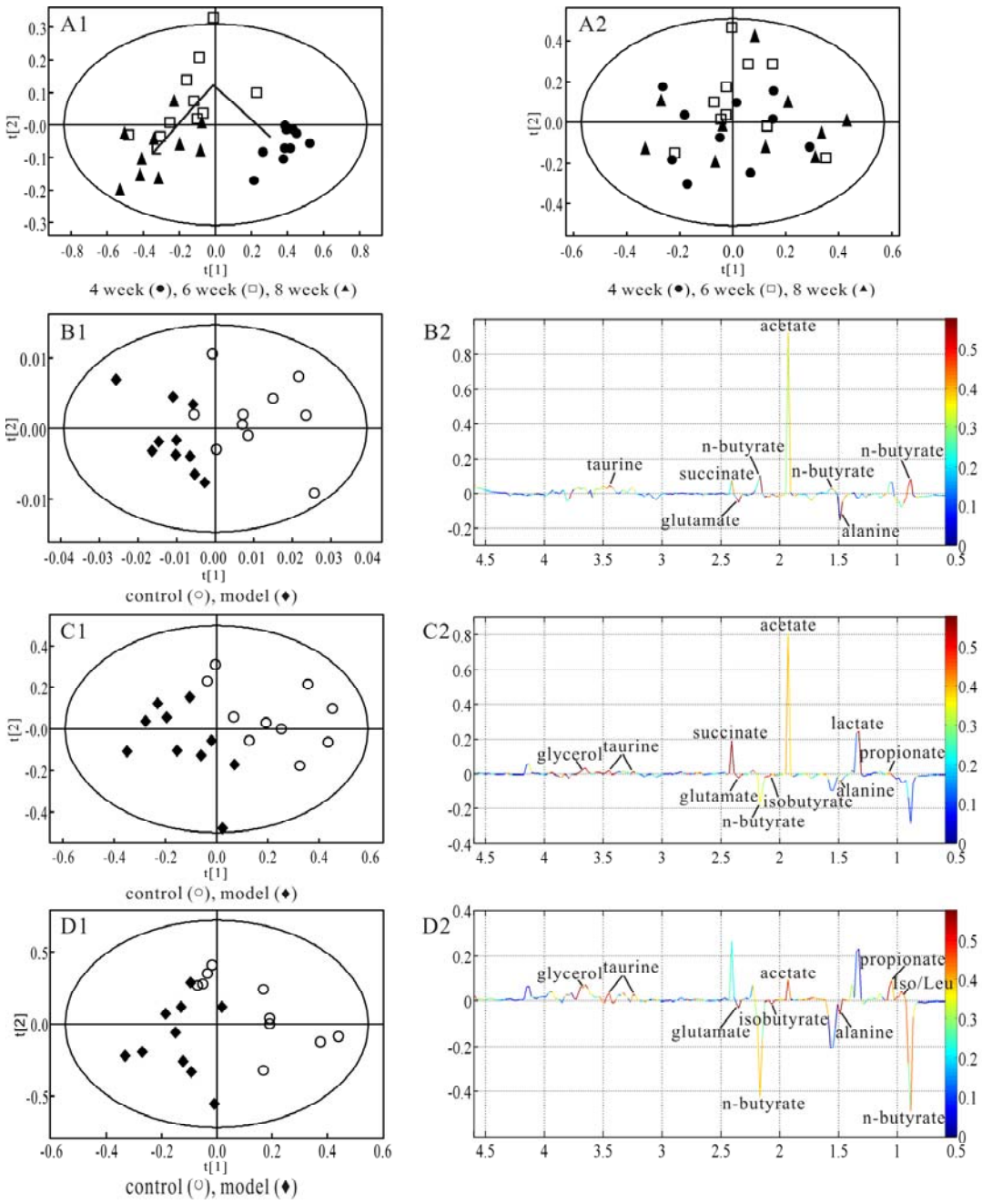

Figure 6 Multivariate data analyses of ^{1}H NMR spectra of fecal extracts at the end of 4th, 6th and 8th week. A1, A2: PCA score plots of IR model (R^2X=62.7%, Q^2=48.4%) and control (R^2X=49.4%, Q^2=23.1%) rats at three time points. B1, B2: Score plot and coefficient-coded loading plot of PLS-DA between control and fructose-fed model groups at the end of 4th week (R^2X=49.7%, Q^2Y=61.7%). C1, C2: Score plot and coefficient-coded loading plot of PLS-DA between control and fructose-fed model groups at the end of 6th week (R^2X=86.5%, Q^2Y=80.8%). D1, D2: Score plot and coefficient-coded loading plot of PLS-DA between control and fructose-fed model groups at the end of 8th week (R^2X=63.1%, Q^2Y=47.8%).

Table 4 summarized the statistical analysis results of the normalized integrals of metabolites screened out in Fig. 6, accounting for the metabolites differentiation between two groups at 4^{th}, 6^{th} and 8^{th} week.

Table 4 The statistical analysis result of the metabolites in fecal extracts of control and model group at 4^{th}, 6^{th} and 8^{th} week.

metabolites	chemical shift	variations		
		4^{th} week	6^{th} week	8^{th} week
n-butyrate	0.90(t)	↓*	↑*	↑*
	1.56(m)			
	2.16(t)			
propionate	1.06(t)	-	↓*	↓**
alanine	1.48(d)	↑*	↑*	↑**
acetate	1.92(s)	↓*	↓*	↓**
glutamate	2.35(m)	↑*	↑**	↑**
succinate	2.41(s)	↓*	↓**	-
taurine	3.27(t)	↓*	↓**	↓**
	3.43(t)			
glycerol	3.65(dd)	-	↓**	↓**

*: to compare with controls * $p<0.05$; ** $p<0.01$.

4. Discussion

The fructose-fed IR models used in our study have been previously found to be appropriate for researching insulin resistance associated with high fructose consumption.[8,9] From Table 1, we found that excessive consumption of fructose induced insulin resistance, which were in accordance with the previous studies.[13] Combined with pattern recognition techniques, we have applied ^{1}H NMR based metabonomics of urine, plasma and fecal extracts to discriminate the fructose-fed IR model group from the control group, suggesting the fructose feeding can intervene in the metabolic network, and induce the metabolic disorders.

The fructose-fed rats were unable to use insulin effectively, leading to impaired glucose uptake and utilization. Consequently, the body would regulate its energy metabolism, resulting in a systemic disorder of energy synthesis and metabolism.[24] The energy needed for the body requires ATP, which primarily originates from glycolysis, glucose and lipid oxidation. Under normal physiological conditions, the substrates of glucose, amino acids, ketone bodies and fatty acids are utilized. However,

fructose feeding decreased glucose metabolism and the sensitivity to normal insulin levels. A number of metabolites involved in energy metabolism were perturbed after fructose treatment. Compared with the control group, the plasma levels of pyruvate and lactate in the model group reduced significantly. This indicated that fructose feeding induced the glycolysis disorders. The NMR spectra showed the continuous decrease of citrate and α-KG in urine, the intermediate products of TCA cycle, which were indicative of alterations in energy metabolism[25,26] and impairments in mitochondrial function.[27] The reduced pyruvate revealed that the generation of acetylcoenzymeA (acetyl-CoA) was down regulated, and resulted in inhibition of Kreb's cycle. Additionally, together with the accumulation of alanine and glycine in plasma, the decreased level of pyruvate probably demonstrated the reduced production from amino acids.

Taurine, possessing many vital properties, such as antioxidation, osmoregulation, membrane stabilization, Ca^{2+} flux regulation, and attenuation of apoptosis,[28-30] decreased in urine and fecal extracts during the whole experiment, while it increased in the plasma at 8^{th} week. Urinary taurine has long been identified as a specific marker of liver toxicity and damage,[31,32] including necrosis and steatosis. Liver is a metabolism place for the maintenance of lipid, glucose, and hormonal homeostasis. As such, the liver is at the crossroads of metabolic health and disease. Fructose feeding has also been shown to induce the activation of carbohydrate regulatory element-binding protein (ChREBP), and to increase the expression of lipogenic genes such as fatty acid synthase (FAS) and acyl coenzyme-A carboxylase (ACC).[33] Long-term fructose intake is associated with nonalcoholic fatty liver disease (NAFLD) which is another manifestation of the metabolic syndrome.[34] Therefore, the metabolic changes of taurine revealed the liver damage and dysfunction induced by excessive

consumption of fructose.[33,34]

Choline is a part of glycerophospholipids, which was activated by choline kinase and phosphocholine cytidylyltransferase. The decreases of choline and PC/GPC, as important constituents of cell membranes, were found in urine at the end of 6th and 8th week, which probably demonstrated the disturbed membrane phospholipid metabolism. Choline was a primary source for methyl groups via one of its metabolites betaine that participates in the synthesis pathways.[35] Betaine was synthesized from glycine. So the decline level of choline probably resulted in accumulation of glycine and betaine in the urine and plasma.

Muscle motion requires a lot of energy, and creatinine is one of the most important materials which is the decomposition of creatine and excreted by kidney. The increased creatine/creatinine was found in fructose-fed rats' urine from 4th week to the end of 8th week compared with the controls. This result suggested that administration of fructose feeding induce the glomerular inflammation and kidney failure. The high level of TMAO, commonly associated with osmotic stress in the renal medulla and a signal of drug-induced nephrotoxicity[36,37] was found in fructose feeding rats. This also revealed the renal injury. The increased level of TMAO in urine from 4th week to 6th week was likely related to the fructose feeding induced disruption in intestinal flora. The reduced level of glycerol in plasma may indicate the fat metabolism disorder caused by the fructose feeding.

Hippurate is normally found in urine, and it is correlated with the microbial activity and composition of the gut.[38,39] An increased level of hippurate in the urine of fructose-fed rats was found at the end of 6th week, which was consistent with the predecessors' study.[40] This change indicated the disorder of gut microbiota under fructose feeding. We found that acetate increased in urine and plasma, while it

decreased in fecal extracts. Acetate is the final product of lipid metabolism and it can be catalyzed to acetyl-Coenzyme A (acetyl-CoA) by acetyl-CoA synthetase.[41] Therefore, the increased level of acetate in urine and plasma reflected an accelerated lipid catabolism as a consequence of perturbed energy metabolism. Acetate, propionate and n-butyrate are the major short chain fatty acids (SCFAs) produced during fermentation by gut bacteria. Dolara et al have demonstrated that lower concentrations of SCFAs in feces are associated with higher rates of colonic mucosal proliferation, which directly related to increased risk of colon cancer.[42] The significant decline of acetate and propionate in fecal extracts suggested that fructose feeding possibly increased the risk of colorectal cancer. N-butyrate is regarded as an important energy source for colonic epithelial cells of the host.[43] SCFAs can reflect the activity and metabolism of intestinal anaerobic bacteria indirectly. Under normal circumstance, only less than 5% of SCFAs will appear in feces. That is because, after being digested and absorbed by small intestine, the digestion will enter the cecum which is rich in carbon and nitrogen source for bacterial fermentation and utilization, and produce a large number of SCFAs in the action of bacteria in cecum. These SCFAs move to the far end direction of colon with the digestion. A large number of SCFAs are reabsorbed by colon in this process. In fecal extracts n-butyrate decreased at 4^{th} week and increased from 6^{th} week to the end of the 8^{th} week, which indicated fructose feeding may induce the intestinal flora disturbance and the colonic re-absorption dysfunction.

A time-dependent increase in the fecal extracts of alanine reveals a higher presence of potential inhibitors of the uracil transporters in the jejunum of fructose-fed rats, which actively transports uracil from mucosa to serum. As one of amino acids to construct protein, glutamate is the very important nutrients in humans and animals.[44] Many factors can affect the levels of glutamate presented in fecal extracts, such as the

absorption of the gut epithelium and the metabolism of gut microbiota. The increased levels of glutamate in fecal extracts possibly suggest the gut epithelium dysfunction and the intestinal flora disorder.

5. Conclusion

^{1}H NMR metabonomics in conjunction with pattern recognition and statistical analyses of urine, plasma and fecal extracts revealed a number of complex disturbances in the endogenous metabolites, which could be related to excessive fructose feeding. Amino acid metabolism, energy and gut microbiota metabolism, together with possible liver and kidney injure, could be affected by fructose feeding. It is concluded that ^{1}H NMR-based metabonomics is a very useful approach for demonstrating the biochemical changes to monitor the progression of IR from a systematic and holistic view.

Acknowledge

We acknowledge the financial supports from the National Natural Science Foundation of China (21005022, 81274059, 81274060, 81073024), and the Guangdong Natural Science Foundation (S2011010002512).

Reference

1 P. Zimmet, K. G. M. M. Alberti and J. Shaw, Nature, 2001, 414, 782-787.

2 S. A. Isezuo, Niger. Postgrad. Med. J., 2006, 13, 247-255.

3 E. J. M. Feskens, S. M. Virtanen, L. Räsänen, J. Tuomilehto, J. Stengård, J. Pekkanen, A. Nissinen and D. Kromhout, Diabetes. Care., 1995, 18, 1104-1112.

4 I. S. Hwang, H. Ho, B. B. Hoffman and G. M. Reaven, Hypertension, 1987, 10, 512-516.

5 H. Basciano, L. Federico and K. Adeli, Nutr. Metab., 2005, 2, 2-5.

6 G. A. Bray, S. J. Nielsen and B. M. Popkin, Am. J. Clin. Nutr., 2004, 79, 537-543.

7 R. Kohen-Avramoglu, A. Theriault and K. Adeli, Clin. Biochem., 2003, 36, 413-420.

8 M. M. Abdullah, N. N. Riediger, Q. L. Chen, Z. H. Zhao, N. Azordegan, Z. Y. Xu, G. Fischer, R. A. Othman, G. N. Pierce, P. S. Tappia, J. T. Zou and M. H. Moghadasian, Mol. Cell. Biochem., 2009, 327, 247-256.

9 H. O. El Mesallamy, E. El-Demerdash, L. N. Hammad and H. M. El Magdoub, Diabetol. Metab. Syndr., 2010, 2, 46-56.

10 F. Hosseini-Esfahani, Z. Bahadoran, P. Mirmiran, S. Hosseinpour-Niazi, F. Hosseinpanah and F. Azizi, Nutr. Metab., 2011, 8, 50-57.

11 B. Cannizzo, A. Lujan, N. Estrella, C. Lembo, M. Cruzado and C. Castro, Exp. Diabetes. Res., 2012, 2012, 1304-1312.

12 F. Briand, Q. Thiéblemont, E. Muzotte and T. Sulpice, J. Nutr., 2012, 142, 704-709.

13 J. K. Nicholson, J. C. Lindon and E. Holmes, Xenobiotica, 1999, 29, 1181-1189.

14 P. Wang, H. Sun, H. T. Lv, W. J. Sun, Y. Yuan, Y. Han, D. W. Wang, A. H. Zhang and X. J. Wang, J. Pharm. Biomed. Anal., 2010, 53, 631-645.

15 P. Bernini, I. Bertini, C. Luchinat, L. Tenori and A. Tognaccini, J. Proteome. Res., 2011, 10, 4983-4992.

16 J. B. Peng, H. M. Jia, T. Xu, Y. T. Liu, H. W. Zhang, L. L. Yu, D. Y. Cai and Z. M. Zou, Process. Biochem., 2011, 46, 2240-2247.

17 M. F. Mahmoud, M. El-Nagar and H. M. El-Bassossy, Arch. Pharm. Res., 2012, 35, 155-162.

18 Y. Zhao, J. F. Wu, J. V. Li, N. Y. Zhou, H. R. Tang and Y. L. Wang, J. Proteome. Res., 2013, 12, 2987-2999.

19 D. Barham and P. Trinder, Analyst, 1972, 97, 142-145.

20 D. R. Matthews, J. P. Hosker, A. S. Rudenski, B. A. Naylor, D. F. Treacher and R. C. Turner, Diabetologia, 1985, 28, 412-419.

21 X. J. Zhao, C. Y. Huang, H. H. Lei, X. Nie, H. R. Tang and Y. L. Wang, J. Proteome. Res., 2011, 10, 5183-5190.

22 J. K. Nicholson, P. J. Foxall, M. Spraul, R. D. Farrant and J. C. Lindon, Anal. Chem., 1995, 67, 793-811.

23 G. Le Gall, S. O. Noor, K. Ridgway, L. Scovell, C. Jamieson, I. T. Johnson, I. J. Colquhoun, E. K. Kemsley and A. Narbad, J. Proteome. Res., 2011, 10, 4208-4218.

24 D. An and B. Rodrigues, Am. J. Physiol. Heart. Circ. Physiol., 2006, 291, 1489–1506.

25 W. J. Cong, Q. L. Liang, L. Li, J. Shi, Q. F. Liu, Y. Feng, Y. M. Wang and G. A. Luo, Talanta, 2012, 89, 91-98.

26 M. X. Yang, S. Wang, F. H. Hao, Y. J. Li, H. R. Tang and X. M. Shi, Talanta, 2012, 88, 136-144.

27 N. J. Waters, C. J. Waterfield, R. D. Farrant, E. Holmes and J. K. Nicholson, Chem. Res. Toxicol., 2005, 18, 639-654.

28 J. H. Wang, H. P. Redmond, R. W. Watson, C. Condron and D. Bouchier-Hayes, Shock, 1996, 6, 331-338.

29 C. Condron, P. Neary, D. Toomey, H. P. Redmond and D. Bouchier- Hayes, Shock, 2003, 19, 564-569.

30 S. G. Maher, C. E. Condron, D. J. Bouchier-Hayes and D. M. Toomey, Clin. Exp. Immunol., 2005, 139, 279–286.

31 C. J. Waterfield, J. A. Turton, M. D. Scales and J. A. Timbrell, Arch. Toxicol., 1993, 67, 244-254.

32 T. A. Clayton, J. C. Lindon, J. R. Everett, C. Charuel, G. Hanton, J. L. Le Net, J. P.

425 Provost and J. K. Nicholson, Arch. Toxicol., 2003, 77, 208-217.
426 33 R. Rodríguez-Calvo, E. Barroso, L. Serrano, T. Coll, R. M. Sánchez, M. Merlos, X.
427 Palomer, J. C. Laguna and M. Vázquez-Carrera, Hepatology., 2009, 49, 106-115.
428 34 X. Ouyang, P. Cirillo, Y. Sautin, S. McCall, J. L. Bruchette, A. M. Diehl, R. J.
429 Johnson and M. F. Abdelmalek, J. Hepatol., 2008, 48, 993-999.
430 35 P. I. Holm, P. M. Ueland, G. Kvalheim and E. A. Lien, Clin. Chem., 2003, 49,
431 286-294.
432 36 J. Feng, X. Li, F. Pei, X. Chen, S. Li and Y. Nie, Analytical. Biochemistry., 2002,
433 301, 1-7.
434 37 P. J. Foxall, G. J. Mellotte, M. R. Bending, J. C. Lindon and J. K. Nicholson,
435 Kidney. International., 1993, 43, 234-245.
436 38 N. G. Psihogios, I. F. Gazi, M. S. Elisaf, K. I. Seferiadis and E. T. Bairaktari,
437 NMR. Biomed., 2008, 21, 195-207.
438 39 L. Wei, P. Q. Liao, H. F. Wu, X. J. Li, F. K. Pei, W. S. Li and Y. J. Wu, Toxicol.
439 Appl. Pharmacol., 2009, 234, 314–325.
440 40 L. C. Zhao, X Liu, L. Y. Xie, H. C. Gao and D. H. Lin, Anal. Sci., 2010, 26,
441 1277-1282.
442 41 S. Kumari, R. Tishel, M. Eisenbach and A. J. Wolfe, J. Bacteriol., 1995, 177,
443 2878-2886.
444 42 P. Dolara, G. Caderni, M. Salvadori, G. Morozzi, R. Fabiani, A. Cresci, C.
445 Orpianesi, G. Trallori, A. Russo and D. Palli, Nutr. Cancer., 2002, 42, 186-190.
446 43 T. L. Miller and M. J. Wolin, Appl. Environ. Microbiol., 1996, 62, 1589-1592.
447 44 G. Andersen, B. Andersen, D. Dobritzsch, K. D. Schnackerz and J. Piskur, FEBS.
448 J., 2007, 274, 1804–1817.